

Girsanov reweighting for metadynamics simulations

Cite as: J. Chem. Phys. **149**, 072335 (2018); <https://doi.org/10.1063/1.5027728>

Submitted: 05 March 2018 . Accepted: 10 July 2018 . Published Online: 27 July 2018

Luca Donati , and Bettina G. Keller 



View Online



Export Citation



CrossMark

ARTICLES YOU MAY BE INTERESTED IN

[Reweighted autoencoded variational Bayes for enhanced sampling \(RAVE\)](#)

The Journal of Chemical Physics **149**, 072301 (2018); <https://doi.org/10.1063/1.5025487>

[Frequency adaptive metadynamics for the calculation of rare-event kinetics](#)

The Journal of Chemical Physics **149**, 072309 (2018); <https://doi.org/10.1063/1.5024679>

[Automated design of collective variables using supervised machine learning](#)

The Journal of Chemical Physics **149**, 094106 (2018); <https://doi.org/10.1063/1.5029972>

Submit Today

**The Journal
of Chemical Physics**

The Emerging Investigators Special Collection and Awards
Recognizing the excellent work of early career researchers!

Girsanov reweighting for metadynamics simulations

Luca Donati^{a)} and Bettina G. Keller^{b)}

Department of Biology, Chemistry, Pharmacy, Freie Universität Berlin, Takustraße 3, D-14195 Berlin, Germany

(Received 5 March 2018; accepted 10 July 2018; published online 27 July 2018)

Metadynamics is a computational method to explore the phase space of a molecular system. Gaussian functions are added along relevant coordinates on the fly during a molecular-dynamics simulation to force the system to escape from minima in the potential energy function. The dynamics in the resulting trajectory are however unphysical and cannot be used directly to estimate dynamical properties of the system. Girsanov reweighting is a recent method used to construct the Markov State Model (MSM) of a system subjected to an external perturbation. With the combination of these two techniques—metadynamics/Girsanov-reweighting—the unphysical dynamics in a metadynamics simulation can be reweighted to obtain the MSM of the unbiased system. We demonstrate the method on a one-dimensional diffusion process, alanine dipeptide, and the hexapeptide Val-Gly-Val-Ala-Pro-Gly (VGVAPG). The results are in excellent agreement with the MSMs obtained from direct unbiased simulations of these systems. We also apply metadynamics/Girsanov-reweighting to a β -hairpin peptide, whose dynamics is too slow to efficiently explore its phase space by direct simulation. Published by AIP Publishing. <https://doi.org/10.1063/1.5027728>

I. INTRODUCTION

Molecular dynamics (MD) simulations yield a realization, \mathbf{x}_t , of the conformational dynamics of a molecular system at atomistic resolution, where $\mathbf{x} \in \Gamma$ is a point in the molecular phase space Γ and t is the time. MD simulations are typically used to estimated phase-space ensemble averages $\mathbb{E}_{\Gamma}[a]$ of observable functions $a(\mathbf{x})$,

$$\mathbb{E}_{\Gamma}[a] = \int_{\Gamma} a(\mathbf{x}) \mu_{\Gamma}(\mathbf{x}) d\mathbf{x}, \quad (1)$$

which can then be interpreted in terms of the underlying phase-space probability density $\mu_{\Gamma}(\mathbf{x})$. Molecular systems are characterized by a vast phase space and high barriers in the potential energy function. Thus, the sampling of the phase-space probability density converges slowly, which renders the estimation of ensemble averages from direct unbiased simulations computationally expensive or even prohibitive for many systems.

A wide range of techniques have been developed to enhance the sampling in MD simulations, such as replica exchange MD,¹ umbrella sampling,² and metadynamics.^{3–6} These simulations yield unphysical trajectories. However, the phase-space ensemble average of the unbiased molecular system can nonetheless be estimated from these trajectories by comparing the phase-space probability densities of the biased and the unbiased system for each frame in the trajectory (phase-space reweighting). The combination of enhanced sampling and phase-space reweighting techniques has increased the system sizes that can be investigated by MD simulations enormously.

It is important to note that the analysis of phase-space ensemble averages only yields information on the relative population of the various conformations of the molecular system but not on the dynamics with which the system transitions between these conformations. In fact, when estimating phase-space ensemble averages from trajectory data, the time-information is completely neglected. In principle, MD trajectories contain the full information of the molecular dynamics. Yet, extracting any interpretable dynamic properties from these data is an intricate task.^{7–11} One property, which can readily be estimated from MD trajectories, is the time-lagged correlation function between two observable functions $a(\mathbf{x})$ and $b(\mathbf{x})$,

$$\text{cor}(a, b; \tau) = \int_{\Gamma} \int_{\Gamma} a(\mathbf{x}) \mu_{\Gamma}(\mathbf{x}) p(\mathbf{x}, \mathbf{y}; \tau) b(\mathbf{y}) d\mathbf{x} d\mathbf{y}, \quad (2)$$

where $p(\mathbf{x}, \mathbf{y}; \tau)$ is the transition probability density, i.e., the probability to find the system at \mathbf{y} after at time $t + \tau$ given that it has been in \mathbf{x} at time t . Markov state models (MSMs)^{12–20} make use of cross-correlation functions to build a transition probability matrix of the dynamics. From the dominant eigenvectors and eigenvalues of the transition probability matrix, one obtains a coarse-grained, and thus humanly understandable, representation of the complex and often multiscalar molecular dynamics. MSMs have become an indispensable tool for the elucidation of complex molecular dynamics and have highlighted the importance of dynamic effects in understanding the function and macroscopic properties of molecular systems.^{21–26}

When constructing MSMs, one faces a similar sampling problem as for the estimation of phase-space ensemble averages. However until a few years ago, MSMs could not be estimated from enhanced sampling simulations because methods to reweight the transition probability density

^{a)}Electronic mail: luca.donati@fu-berlin.de

^{b)}Electronic mail: bettina.keller@fu-berlin.de

$p(\mathbf{x}, \mathbf{y}; \tau)$ from the biased dynamics to the unbiased dynamics were lacking. Although protocols to optimally seed²⁷ and respawn²⁸ simulations have been proposed, the limitation to unbiased simulations made MSMs computationally very expensive.

In recent years, several dynamic reweighting schemes^{32–36} have been published with which one can reweight a discrete approximation of the transition probability density, namely, $\mathbb{P}[\mathbf{x}_{t+\tau} \in B_j | \mathbf{x}_t \in B_i]$, the conditional probability of finding the system within state B_j at time $t + \tau$, given that it has been in state B_i at time t . $B_i, B_j \subset \Gamma$ are discrete states in the phase space of the system. These methods need to assume that the system is in local equilibrium within state B_i before it transitions to state B_j .

An alternative approach is the Girsanov reweighting method for path ensemble averages,^{37–39} in which not the transition probability $\mathbb{P}[\mathbf{x}_{t+\tau} \in B_j | \mathbf{x}_t \in B_i]$ but the transition probability density $p(\mathbf{x}, \mathbf{y}; \tau)$ is reweighted. One advantage of this approach is that one does not need to assume local equilibrium or even the prior definition of a particular discretization of the molecular phase space. Reweighting $p(\mathbf{x}, \mathbf{y}; \tau)$ becomes possible by considering the ensemble of all possible paths $\omega = \{\mathbf{x}_0, \mathbf{x}_1, \dots, \mathbf{x}_n\}$ of length τ which start in point \mathbf{x}_0 at time t and end in point $\mathbf{x}_n = \mathbf{y}$ at time $t + \tau$. Then, instead of reweighting the transition probability as such, the probability density with which each individual path occurs is reweighted from the biased dynamics to the unbiased dynamics. Integrating over the path ensemble with appropriately reweighted path probability densities ultimately yields the transition probability density of the unbiased system.

We have recently demonstrated the Girsanov reweighting method for all-atom MD simulations and used it to reweight MSMs from a reference potential energy function to a series of perturbed potential energy functions.³⁹ Since the transition probability density $p(\mathbf{x}, \mathbf{y}; \tau)$ is reweighted, the Girsanov reweighting method can be applied to reweighted arbitrary correlation functions [Eq. (2)] and to obtain the associated dynamic properties, such as, for example, stopping times of trajectories which reach a certain target set.⁴⁰

In this contribution, we ask whether Girsanov reweighting can be used to obtain unbiased MSMs from simulations which are biased by a metadynamics potential. Metadynamics^{3–6} is an enhanced sampling method, in which Gaussian functions are deposited along collective variables such that the system is driven out of the minima of the potential energy function. When fully converged, the metadynamics potential compensates the free energy surface in the space of the collective variables. Thus, the bias is quite strong. On the other hand, the variance of the Girsanov reweighting estimator sensitively depends on the gradient of the bias. We choose a heuristic approach and test whether a biasing strength which yields an appreciable speed-up of the simulation is compatible with the Girsanov reweighting method. First, we benchmark the biasing strength and the metadynamics/Girsanov-reweighting method on a one-dimensional diffusion process. Then, we demonstrate the method on two molecular systems for which reference MSMs can be constructed by direct simulation (alanine dipeptide and a hexapeptide). Finally, we use metadynamics/Girsanov-reweighting to obtain a MSM of a

β -hairpin peptide whose dynamics is too slow to obtain a MSM by direct simulation.

II. THEORY

A. Molecular dynamics

Consider a molecular system governed by the Langevin equation,

$$\begin{aligned} M \frac{d\mathbf{v}(t)}{dt} &= -\nabla V_t(\mathbf{r}(t)) - \gamma \mathbf{v}(t) + \sigma \eta(t), \\ \mathbf{v}(t) &= \frac{d\mathbf{r}(t)}{dt}, \end{aligned} \quad (3)$$

where M is the mass matrix, $\mathbf{r}(t)$ and $\mathbf{v}(t) \in \mathbb{R}^{3N}$ are the position and the velocity vector. $V_t(\mathbf{r})$ is the potential energy function, which may be time-dependent. The interaction between the molecular system and the solvent is modeled by the friction coefficient γ and an uncorrelated Gaussian white noise $\eta(t) \in \mathbb{R}^{3N}$, which is scaled by the volatility σ according to the Einstein relation $\sigma = \sqrt{2k_B T \gamma M}$ where k_B is the Boltzmann constant and T is the temperature of the system. The state of the system at time t is represented by the vector $\mathbf{x}(t) = \{\mathbf{r}(t), \mathbf{v}(t)\} \in \Gamma$, where $\Gamma = \mathbb{R}^{6N}$ denotes the phase space of the system.

Numerical integration of Eq. (3) with a time step of Δt for n time steps yields a time-discretized trajectory $\omega = \{\mathbf{x}_0, \mathbf{x}_1, \dots, \mathbf{x}_n\}$. Note that the numerical integration requires a sequence of normal random numbers for each dimension of the position space $\eta^{(i)} = \{\eta_1^{(i)}, \dots, \eta_n^{(i)}\}$, with $\eta_k^{(i)} \sim \mathcal{N}(0, 1)$ and $i \in [1, 2, \dots, \mathbb{R}^{3N}]$.

B. Metadynamics

A recurrent problem in MD simulations is that one needs to generate very long trajectories to exhaustively sample the phase space Γ . Metadynamics^{3,4} is a technique used to accelerate the exploration of the phase-space along a few relevant coordinates (also known as collective variables) along which the slowest transitions in the system occur. We consider a set of d collective variables $s = s(\mathbf{r}) = \{s_1(\mathbf{r}), s_2(\mathbf{r}), \dots, s_d(\mathbf{r})\}$. During the build-up phase in metadynamics, a time-dependent potential $V_{\text{meta}}(s, t)$ is added to a reference potential $V_0(\mathbf{r})$, and Eq. (3) is integrated with

$$V_t(\mathbf{r}) = V_0(\mathbf{r}) + V_{\text{meta}}(s(\mathbf{r}), t). \quad (4)$$

Thus, this build-up phase corresponds to a simulation of Langevin dynamics with a time-dependent potential energy function. The biasing potential is constructed as a growing sum of Gaussian functions on the collective variables s_i as

$$V_{\text{meta}}(s, t) = \sum_{t'=\tau_G, 2\tau_G, \dots}^{t'<t} W \exp\left(-\sum_i^d \frac{(s_i - s_i(\mathbf{r}(t')))^2}{2\sigma_{s_i}^2}\right), \quad (5)$$

where W is the height of the Gaussian, and σ_{s_i} is the variance of the Gaussian function along the collective variable s_i . At regular intervals τ_G , the biasing potential is updated by adding a Gaussian function of width σ_{s_i} , which is centered at the current position $\mathbf{r}(t')$, to the current potential. Note that the parameter τ_G is not related to the Markov model lag-time τ . The effect is that already visited positions are discouraged and the system

is driven out of the minima of the original energy potential. In the long time limit, the biasing potential converges to minus the free energy F profile along the collective variable $V_{\text{meta}}(s, t \rightarrow \infty) = -F(s) + C$, where C is a constant.

Well-tempered metadynamics is a variant of metadynamics, in which the height of each Gaussian function W in Eq. (5) is scaled according to

$$W(t') = W_0 \exp\left(-\frac{V_{\text{meta}}(s, t')}{\Delta T}\right), \quad (6)$$

where W_0 is the height of the Gaussian at $V_{\text{meta}}(s, t) = 0$ and ΔT is a temperature-like parameter that controls the decay rate of W . The higher the current metadynamics potential $V_{\text{meta}}(s, t)$ at a position s , the smaller the height of the newly added Gaussian functions. In the long time limit, the well-tempered metadynamics potential [Eq. (5)] does not fully compensate the free energy profile but converges to

$$V_{\text{meta}}(s, t \rightarrow \infty) = -\frac{\Delta T}{T + \Delta T} F(s) + C, \quad (7)$$

while the probability distribution on collective variables converges to

$$\pi(s) \propto \exp\left[-\beta\left(\frac{T}{T + \Delta T} F(s)\right)\right]. \quad (8)$$

Note that ΔT controls the extent to which $V_{\text{meta}}(s, t \rightarrow \infty)$ compensates the free-energy profile. For $\Delta T \rightarrow +\infty$, $W \rightarrow W_0$ and the standard metadynamics is retained, while for $\Delta T \rightarrow 0$, unbiased MD is recovered.

Various reweighting schemes^{41–44} have been developed to estimate phase-space ensemble averages of the reference potential V_0 from the biased simulation. Note, however, that typically the *build-up* phase of a metadynamics simulation, i.e., the part of the simulation in which the metadynamics potential grows, is not analyzed due to the difficulties that arise in analyzing dynamics at time-dependent potential energy functions. Instead, the converged metadynamics potential $V_{\text{meta}}(s, \mathbf{r})$ is used to construct a time-independent potential energy function

$$V(\mathbf{r}) = V_0(\mathbf{r}) + V_{\text{meta}}(s, \mathbf{r}). \quad (9)$$

MD simulation at this potential is carried out and analyzed by phase-space reweighting methods. We will call this latter type of simulation metadynamics *rerun*.

C. Markov state models

Consider a dynamic process which is Markovian, ergodic, and reversible, such as Eq. (3). The time-evolution of the associated phase-space probability density $p_t(\mathbf{x})$ can be represented by a *propagator* $\mathcal{P}(\tau)$, a continuous operator that transports the probability density forward in time: $p_{t+\tau}(\mathbf{y}) = \mathcal{P}(\tau)p_t(\mathbf{x}) = \int_{\Gamma} p(\mathbf{x}, \mathbf{y}; \tau)p_t(\mathbf{x}) d\mathbf{x}$. This propagator can be approximated by Markov state models (MSM).^{12–18,20}

In MSMs, the phase space is discretized into g disjoint sets (or microstates) B_1, B_2, \dots, B_g with $\cup_{i=1}^g B_i = \Gamma$. Given a lag-time τ , the probability of observing a transition from B_i to B_j , $\mathbb{P}[\mathbf{x}_n \in B_j, \mathbf{x}_0 \in B_i]$, can be represented by a cross-correlation function

$$C_{ij}(\tau) = \int_{\Gamma} \int_{\Gamma} \mathbf{1}_{B_i}(\mathbf{x}) \mu_{\Gamma}(\mathbf{x}) \mathbf{1}_{B_j}(\mathbf{y}) p(\mathbf{x}, \mathbf{y}; \tau) d\mathbf{y} d\mathbf{x}, \quad (10)$$

where $\mathbf{1}_{B_i}$ is the indicator function of the i th set

$$\mathbf{1}_{B_i}(\mathbf{x}) := \begin{cases} 1 & \text{if } \mathbf{x} \in B_i \\ 0 & \text{otherwise} \end{cases}, \quad (11)$$

and $\mu_{\Gamma}(\mathbf{x})$ is the stationary probability density

$$\mu_{\Gamma}(\mathbf{x}) = \frac{\exp[-\beta \mathcal{H}(\mathbf{x})]}{Z}, \quad (12)$$

where $\beta = \frac{1}{k_B T}$, $\mathcal{H}(\mathbf{x}) = \frac{1}{2} \mathbf{v}^T M \mathbf{v} + V(\mathbf{r})$ is the classical Hamiltonian of the system, and $Z = \int_{\Gamma} \exp[-\beta \mathcal{H}(\mathbf{x})] d\mathbf{x}$ is the partition function.

The conditional transition probability $\mathbb{P}[\mathbf{x}_n \in B_j | \mathbf{x}_0 \in B_i]$ of observing the system in B_j at time $t + \tau$, given that it has been in B_i at time t , is

$$T_{ij}(\tau) = \frac{C_{ij}(\tau)}{\sum_{j=1}^g C_{ij}(\tau)}. \quad (13)$$

For reversible processes, the resulting transition matrix $\mathbf{T}(\tau)$: $T_{ij}(\tau)$ is a matrix representation (approximation) of the propagator. Its dominant eigenvectors and eigenvalues contain information about the slow processes of the system,^{12–18,20}

$$\begin{aligned} \mathbf{T}(\tau) \mathbf{r}_k &= \lambda_k(\tau) \mathbf{r}_k, \\ \mathbf{l}_k^T \mathbf{T}(\tau) &= \lambda_k(\tau) \mathbf{l}_k^T, \end{aligned} \quad (14)$$

where \mathbf{l}_k^T denotes the transpose of vector \mathbf{l}_k . If the implied time scales

$$t_k(\tau) = -\frac{\tau}{\ln(\lambda_k(\tau))} = \text{const. } \forall \tau > 0 \quad (15)$$

are independent of the lag time τ , the approximation is considered to be valid. In practice, one aims at finding a region of τ , for which the implied time scales are roughly constant.^{15,18}

D. Girsanov reweighting

Girsanov reweighting³⁷ is a method to reweight a path ensemble average $\mathbb{E}_{\Omega}[f]$ which has been measured for dynamics at potential $V(\mathbf{r})$ to its corresponding value at $V(\mathbf{r}) + U(\mathbf{r})$, without re-sampling the dynamics at $V(\mathbf{r}) + U(\mathbf{r})$. Because Eq. (10) can be formulated in terms of a path ensemble average, Girsanov reweighting can be used to obtain the MSM for dynamics at $V(\mathbf{r}) + U(\mathbf{r})$ by reweighting trajectories sampled at $V(\mathbf{r})$.^{38,39} We will explain the method using time-discretized paths ω which are obtained by numerical integrating equation (3). For more details on path spaces and path probabilities and the implications of using time-discrete rather than time-continuous paths, see Ref. 39.

Let $\omega = \{\mathbf{x}_0 = \mathbf{x}, \mathbf{x}_1, \dots, \mathbf{x}_n\}$ be a path of length $\tau = n \cdot \Delta t$ which starts in a specific state $\mathbf{x}_0 = \mathbf{x}$. The path space, i.e., the set of all possible paths ω of length τ which start in $\mathbf{x}_0 = \mathbf{x}$, is $\Omega_{\tau, \mathbf{x}}$. The path probability density, i.e., the probability of observing a path $\omega \in \Omega_{\tau, \mathbf{x}}$, is $\mu_{\Omega}(\omega) = \mu_{\Omega}(\mathbf{x}_1, \mathbf{x}_2, \dots, \mathbf{x}_n | \mathbf{x}_0 = \mathbf{x})$. Let $S_{\tau, \mathbf{x}, m} = \{\omega_1, \omega_2, \dots, \omega_m\} \subset \Omega_{\tau, \mathbf{x}}$ be a sample of the path space, which has been generated by integrating equation (3) with $V_t(\mathbf{r}) = V(\mathbf{r})$ and $\mathbf{x}_0 = \mathbf{x}$. The probability density that a particular path appears in the set is given by $\mu_{\Omega}(\omega)$. Let furthermore $f(\omega) = f(\mathbf{x}_1, \mathbf{x}_2, \dots, \mathbf{x}_n)$ be a path observable, i.e., a function which assigns a real-valued number to each path ω . The path ensemble average of $f(\omega)$ for dynamics at $V(\mathbf{r})$ is

obtained by a weighted integration over all paths, except for the first state $\mathbf{x}_0 = \mathbf{x}$,

$$\begin{aligned} \mathbb{E}_{\Omega}[f | \mathbf{x}_0 = \mathbf{x}] &= \int_{\Omega_{\tau,x}} \mu_{\Omega}(\omega) f(\omega) d\omega \\ &= \int_{\Gamma} \int_{\Gamma} \dots \int_{\Gamma} \mu_{\Omega}(\mathbf{x}_1, \mathbf{x}_2, \dots, \mathbf{x}_n | \mathbf{x}_0 = \mathbf{x}) \\ &\quad \times f(\mathbf{x}_1, \mathbf{x}_2, \dots, \mathbf{x}_n) d\mathbf{x}_1 d\mathbf{x}_2 \dots d\mathbf{x}_n \\ &= \lim_{m \rightarrow \infty} \frac{1}{m} \sum_{\omega_k \in S_{\tau,x,m}} f(\omega_k). \end{aligned} \quad (16)$$

The last equality only holds if the sampling is ergodic. Dynamics at an altered potential $V(\mathbf{r}) + U(\mathbf{r})$ generate a different path probability density $\tilde{\mu}_{\Omega}(\omega)$ and a different path ensemble average $\tilde{\mathbb{E}}_{\Omega}[f | \mathbf{x}_0 = \mathbf{x}]$. However, if the path probability ratio $M_{\tau,x}(\omega) = \tilde{\mu}_{\Omega}(\omega)/\mu_{\Omega}(\omega)$ is defined, $\tilde{\mathbb{E}}_{\Omega}[f | \mathbf{x}_0 = \mathbf{x}]$ can be estimated from the set of paths $S_{\tau,x,m}$ sampled at $V(\mathbf{r})$,

$$\begin{aligned} \tilde{\mathbb{E}}_{\Omega}[f | \mathbf{x}_0 = \mathbf{x}] &= \int_{\Omega_{\tau,x}} \tilde{\mu}_{\Omega}(\omega) f(\omega) d\omega \\ &= \int_{\Omega_{\tau,x}} M_{\tau,x}(\omega) \mu_{\Omega}(\omega) f(\omega) d\omega \\ &= \lim_{m \rightarrow \infty} \frac{1}{m} \sum_{\omega_k \in S_{\tau,x,m}} M_{\tau,x}(\omega_k) f(\omega_k). \end{aligned} \quad (17)$$

The Girsanov theorem specifies the conditions under which $M_{\tau,x}(\omega)$ exists and asserts that

$$\begin{aligned} M_{\tau,x}(\omega) &= \frac{\mu_{\tilde{\Omega}}(\omega)}{\mu_{\Omega}(\omega)} = \exp \left\{ \sum_{i=1}^{3N} \left[\sum_{k=0}^n \frac{\nabla_i U(\mathbf{r}_k)}{\sigma} \eta_k^i \sqrt{\Delta t} \right. \right. \\ &\quad \left. \left. - \frac{1}{2} \sum_{k=0}^n \left(\frac{\nabla_i U(\mathbf{r}_k)}{\sigma} \right)^2 \Delta t \right] \right\}, \end{aligned} \quad (18)$$

where η_k^i are the random numbers, along dimension i at time step k , generated to integrate equation (3) with $V(\mathbf{r})$, and $\nabla_i U(\mathbf{r}_k)$ is the gradient of $U(\mathbf{r})$ along dimension i measured at the position \mathbf{r}_k .

E. Girsanov reweighting for MSMs

To use the Girsanov reweighting method on MSMs, the cross-correlation function [Eq. (10)] has to be reformulated as a path ensemble average. The transition probability $p(\mathbf{x}, \mathbf{y}; \tau)$ in Eq. (10) is obtained from the path probability density $\mu_{\Omega}(\omega)$ by integrating over all intermediate states between $\mathbf{x}_0 = \mathbf{x}$ and $\mathbf{x}_n = \mathbf{y}$,

$$\begin{aligned} p(\mathbf{x}, \mathbf{y}; \tau) &= \int_{\Gamma} \int_{\Gamma} \dots \int_{\Gamma} \mu_{\Omega}(\mathbf{x}_1, \mathbf{x}_2, \dots, \mathbf{x}_n | \mathbf{x}_0 = \mathbf{x}) \\ &\quad \times d\mathbf{x}_1 d\mathbf{x}_2 \dots d\mathbf{x}_{n-1}. \end{aligned} \quad (19)$$

The indicator function of the final set B_j can be regarded as a path observable $f(\omega) = f(\mathbf{x}_n) = \mathbf{1}_{B_j}(\mathbf{x}_n) = \mathbf{1}_{B_j}(\mathbf{y})$. Thus, the integral over the final states \mathbf{y} in Eq. (10) is formally a path ensemble average,

$$\begin{aligned} \int_{\Gamma} p(\mathbf{x}, \mathbf{y}; \tau) \mathbf{1}_{B_j}(\mathbf{y}) d\mathbf{y} &= \int_{\Gamma} \left[\int_{\Gamma} \int_{\Gamma} \dots \int_{\Gamma} \mu_{\Omega}(\mathbf{x}_1, \mathbf{x}_2, \dots, \mathbf{x}_n | \mathbf{x}_0 = \mathbf{x}) \right. \\ &\quad \times d\mathbf{x}_1 d\mathbf{x}_2 \dots d\mathbf{x}_{n-1} \left. \right] \mathbf{1}_{B_j}(\mathbf{x}_n) d\mathbf{x}_n, \end{aligned} \quad (20)$$

$$= \mathbb{E}_{\Omega}[\mathbf{1}_{B_j} | \mathbf{x}_0 = \mathbf{x}]. \quad (21)$$

The integral over the initial states in Eq. (10) is then formally a phase-space ensemble average [Eq. (1)] of an observable function $a(\mathbf{x}) = \mathbf{1}_{B_i}(\mathbf{x}) \mathbb{E}_{\Omega}[\mathbf{1}_{B_j} | \mathbf{x}_0 = \mathbf{x}]$,

$$\begin{aligned} C_{ij}(\tau) &= \int_{\Gamma} \mu_{\Gamma}(\mathbf{x}) \mathbf{1}_{B_i}(\mathbf{x}) \int_{\Omega_{\tau,x}} \mu_{\Omega}(\omega) \mathbf{1}_{B_j}(\mathbf{x}_n) d\omega d\mathbf{x} \\ &= \mathbb{E}_{\Gamma}[\mathbf{1}_{B_i}(\mathbf{x}) \mathbb{E}_{\Omega}[\mathbf{1}_{B_j} | \mathbf{x}_0 = \mathbf{x}]]. \end{aligned} \quad (22)$$

The correlation function is thus a nested combination of a path ensemble average and a phase-space ensemble average. To obtain the correlation function $\tilde{C}_{ij}(\tau)$ at $V(\mathbf{r}) + U(\mathbf{r})$, one needs to reweight the path ensemble average $\mathbb{E}_{\Omega}[\mathbf{1}_{B_j} | \mathbf{x}_0 = \mathbf{x}]$ using Eqs. (17) and (18) and the phase-space ensemble average according to

$$\tilde{\mathbb{E}}_{\Gamma}[a] = \int_{\Gamma} \tilde{\mu}_{\Gamma}(\mathbf{x}) a(\mathbf{x}) d\mathbf{x} = \int_{\Gamma} g(\mathbf{x}) \mu_{\Gamma}(\mathbf{x}) a(\mathbf{x}) d\mathbf{x}, \quad (23)$$

where

$$g(\mathbf{x}) = \frac{\tilde{\mu}_{\Gamma}(\mathbf{x})}{\mu_{\Gamma}(\mathbf{x})} = \frac{Z}{\tilde{Z}} \exp(-\beta U(\mathbf{r})). \quad (24)$$

The function $g(\mathbf{x})$ is the probability ratio of the two phase-space probability densities: $\mu_{\Gamma}(\mathbf{x})$ associated with $V(\mathbf{r})$ and $\tilde{\mu}_{\Gamma}(\mathbf{x})$ associated with $V(\mathbf{r}) + U(\mathbf{r})$. Thus,

$$\begin{aligned} \tilde{C}_{ij}(\tau) &= \int_{\Gamma} \tilde{\mu}_{\Gamma}(\mathbf{x}) \mathbf{1}_{B_i}(\mathbf{x}) \int_{\Omega_{\tau,x}} \tilde{\mu}_{\Omega}(\omega) \mathbf{1}_{B_j}(\mathbf{x}_n) d\omega d\mathbf{x} \\ &= \int_{\Gamma} g(\mathbf{x}) \mu_{\Gamma}(\mathbf{x}) \mathbf{1}_{B_i}(\mathbf{x}) \int_{\Omega_{\tau,x}} M_{\tau,x}(\omega) \mu_{\Omega}(\omega) \mathbf{1}_{B_j}(\mathbf{x}_n) d\omega d\mathbf{x}. \end{aligned} \quad (25)$$

In praxis, $C_{ij}(\tau)$ is estimated from a set of m paths of length τ , $S_{\tau,m} = \{\mathbf{v}_1, \mathbf{v}_2, \dots, \mathbf{v}_m\}$, sampled at $V(\mathbf{r})$ with initial states distributed according to Eq. (12) as

$$C_{ij}(\tau) = \lim_{m \rightarrow \infty} \frac{1}{m} \sum_{k=1}^m \mathbf{1}_{B_i}([\mathbf{x}_0]_k) \cdot \mathbf{1}_{B_j}([\mathbf{x}_n]_k), \quad (26)$$

where $[\mathbf{x}_i]_k$ denotes the i th time step of the k th path. $\tilde{C}_{ij}(\tau)$ can be estimated from the same set of paths by reweighting Eq. (26) analogously to Eq. (25),

$$\tilde{C}_{ij}(\tau) = \lim_{m \rightarrow \infty} \frac{1}{m} \sum_{v_k \in S_{\tau,m}} g([\mathbf{x}_0]_k) \mathbf{1}_{B_i}([\mathbf{x}_0]_k) \cdot M_{\mathbf{x},\tau}(v_k) \mathbf{1}_{B_j}([\mathbf{x}_n]_k). \quad (27)$$

Finally, the transition probability between set B_i and set B_j for the perturbed dynamics is obtained as

$$\tilde{T}_{ij}(\tau) = \frac{\tilde{C}_{ij}(\tau)}{\sum_j \tilde{C}_{ij}(\tau)}. \quad (28)$$

The functions $g(\mathbf{x})$ and $M_{\tau,x}(\omega)$ are two Radon-Nikodym derivatives.³⁷ In particular, $g(\mathbf{x})$ represents a change of measure on the phase-space, while $M_{\tau,x}(\omega)$ represents a change of measure on the path-space.

F. Metadynamics/Girsanov reweighting

The metadynamics/Girsanov-reweighting method consists of running metadynamics simulations and constructing MSMs of the unbiased system by reweighting to the molecular reference potential energy function $V_0(\mathbf{r})$. In rerun metadynamics, the paths $S_{\tau,m} = \{\nu_1, \nu_2, \dots, \nu_m\}$ are sampled at the time-independent potential given by Eq. (9). One would like to reweight the resulting paths to the dynamics at $V(\mathbf{r}) + U(\mathbf{r}) = V_0(\mathbf{r})$. Thus, the perturbation which enters Eq. (18) is

$$U(\mathbf{r}) = V_0(\mathbf{r}) - V(\mathbf{r}) = -V_{\text{meta}}(\mathbf{r}). \quad (29)$$

A different application of the Girsanov reweighting to metadynamics simulations exploits the fact that the Girsanov theorem can also be used to reweight path ensembles generated by time-dependent potential energy functions. Thus, it can be used to reweight the build-up phase of the metadynamics potential. The perturbation which enters Eq. (18) is then time-dependent and is given as

$$U(\mathbf{r}, t) = V_0(\mathbf{r}) - V(\mathbf{r}, t) = -V_{\text{meta}}(\mathbf{r}, t). \quad (30)$$

Additionally, the phase-space probability ratio [Eq. (24)] becomes time-dependent,

$$g(\mathbf{x}, t) = \frac{\tilde{\mu}_\Gamma(\mathbf{x})}{\mu_\Gamma(\mathbf{x}, t)} = \frac{Z}{\tilde{Z}} \exp(\beta V_{\text{meta}}(\mathbf{r}, t)). \quad (31)$$

III. METHODS

A. One-dimensional system

We consider a one-dimensional diffusion process x_t , which is governed by the stochastic differential equation,

$$dx_t = -\nabla V(x_t) + \sigma dB_t, \quad (32)$$

where B_t denotes a standard Brownian motion, $\sigma = 1.5$ is the volatility, and $V(x)$ is a one-dimensional potential energy surface given by the function

$$V(x) = 4\left(x^3 - \frac{3}{2}x\right)^2 - x^3 + x. \quad (33)$$

TABLE I. Implied time scales associated with the second and third MSM eigenvector of the one-dimensional diffusion process. The numbers show the average and standard deviation of a sample of 50 numerical experiments (simulation and reweighted MSM).

| Simulation | | Rerun | Rerun | Rerun | Rerun | |
|------------|-------------------|----------------------|----------------------|----------------------|----------------------|--------------|
| Time steps | Direct simulation | $V_{\text{meta}4e4}$ | $V_{\text{meta}4e5}$ | $V_{\text{meta}4e6}$ | $V_{\text{meta}4e7}$ | Build-up |
| 4e4 | 1.5e3 ± 316 | 1.5e3 ± 415 | 1.61e3 ± 433 | 1.49e3 ± 309 | 1.74e3 ± 530 | 1.53e3 ± 142 |
| | 345 ± 60 | 344 ± 60 | 353 ± 59 | 346 ± 50 | 391 ± 174 | 350 ± 48 |
| 4e5 | 1.53e3 ± 118 | 1.53e3 ± 107 | 1.49e3 ± 81 | 1.51e3 ± 86 | 1.57e3 ± 581 | 1.53e3 ± 76 |
| | 357 ± 18 | 357 ± 17 | 355 ± 15 | 357 ± 17 | 381 ± 146 | 358 ± 16 |
| 4e6 | 1.52e3 ± 32 | 1.52e3 ± 34 | 1.52e3 ± 32 | 1.52e3 ± 21 | 1.5e3 ± 82 | 1.52e3 ± 26 |
| | 357 ± 6 | 357 ± 5 | 357 ± 4 | 357 ± 4 | 347 ± 66 | 358 ± 5 |
| 4e7 | 1.53e3 ± 11 | ... | ... | ... | ... | ... |
| | 358 ± 2 | ... | ... | ... | ... | ... |

This function describes a one-dimensional triple-well potential. Equation (32) has been numerically integrated using the Euler-Maruyama scheme

$$x_{n+1} = x_n - \nabla_x V(x_n) \Delta t + \sigma \eta \sqrt{\Delta t}, \quad (34)$$

where $\Delta t = 0.001$ is the integration time step, η are independent and identically distributed random variables drawn from a standard Gaussian distribution, and n is the index of the time step.

Direct simulations. We have first produced trajectories of 4e4, 4e5, 4e6, and 4e7 time steps. For each trajectory, we built an MSM with enforced detailed balance, extracted the dominant eigenvalues and eigenvectors, and estimated the implied time scales [Eq. (15)] in the range of [10 : 500] time steps. The MSMs were built by discretizing the interval $x = -2 : 2$ in 100 bins. The reference MSM is constructed on the trajectory of 4e7 time steps with a lag-time of 50 time steps. To obtain estimates of the uncertainties in the implied time scales, we repeated each numerical experiment, i.e., simulation and MSM construction, 50 times. Thus, for each of the considered simulation lengths (4e4, 4e5, 4e6, and 4e7), we have 50 trajectories and the associated MSMs. The implied time scales in the column “Direct simulation” Table I are given as the average for each sample of 50 MSMs, and the uncertainties are given as the standard deviation.

Metadynamics build-up. The metadynamics potential $V_{\text{meta}}(s(\mathbf{r}))$ [Eq. (5)] was generated with parameters $W = 0.02$, $\sigma_s = 0.2$, and $\tau_G = 2000$, where $s(\mathbf{r}) = x$. Because $V_{\text{meta}}(s(\mathbf{r}))$ is a sum over Gaussians, the gradient calculation becomes computationally demanding as the number of terms in the sum grows. To overcome this problem and keep the efficiency of the simulation constant, we stored the bias at each update, on a grid of 1000 bins between $x = -2.0$ and $x = 2.0$. We terminated the build-up after 4e4 time steps ($V_{\text{meta}4e4}(x)$), 4e5 time steps ($V_{\text{meta}4e5}(x)$), 4e6 time steps ($V_{\text{meta}4e6}(x)$), and 4e7 time steps ($V_{\text{meta}4e7}(x)$) to obtain four different metadynamics potentials for the metadynamics rerun experiments. We reweighted the trajectory from each of the build-up phases using Eqs. (30) and (31) and obtained an MSM of the unbiased potential [Eq. (33)]. The MSMs were constructed analogously to the MSMs of the direct simulation. As before, we repeated

each numerical experiment, i.e., metadynamics build-up simulation and Girsanov-reweighted MSM, 50 times to obtain averages and standard deviations of the implied time scales (column “Build-up” in Table I).

Metadynamics rerun. We sampled the four metadynamics potentials ($V_{\text{meta}4e4}(x)$, $V_{\text{meta}4e5}(x)$, $V_{\text{meta}4e6}(x)$, $V_{\text{meta}4e7}(x)$) by conducting simulations of 4e4, 4e5, 4e6, and 4e7 time steps for each potential. We reweighted each trajectory using Eq. (29) and obtained an MSM of the unbiased potential [Eq. (33)]. The MSMs were constructed analogously to the MSMs of the direct simulation. In total, this yielded 16 different numerical experiments (metadynamics rerun simulation and Girsanov-reweighted MSM). As before, we repeated each numerical experiment 50 times to obtain averages and standard deviations of the implied time scales (column $V_{\text{meta}4e4}$ to $V_{\text{meta}4e7}$ in Table I).

To numerically integrate Eq. (32) and to build the MSM, we have written our own software in C++.

B. MD simulations

We performed MD simulations of acetyl-alanine-methylamide (Ac-A-NHMe, alanine dipeptide), VGVAPG hexapeptide, and a β -hairpin structure, in implicit water. All simulations were carried out with the OpenMM 7.01 simulation package⁴⁵ in an NVT ensemble at 300 K. Each system was simulated with the force field AMBER ff-14sb⁴⁶ and the GBSA model⁴⁷ for implicit solvent simulation. A Langevin thermostat has been applied to control the temperature and a Langevin leapfrog integrator⁴⁸ has been used to integrate Eq. (3) with a time step of 2 fs. Interactions beyond 1 nm are truncated. Metadynamics has been implemented through the plugin Plumed2.⁶

Girsanov reweighting has been efficiently implemented in OpenMM. We have estimated on the fly the terms of the stochastic and the Riemann integral that appear in Eq. (18), writing out the terms

$$I(a) = \sum_{i=1}^{3N} \sum_{k=(a-1)\cdot\text{nstxout}}^{a\cdot\text{nstxout}-1} \frac{\nabla_i U(\mathbf{r}_k)}{\sigma} \eta_k^i \sqrt{\Delta t} \quad (35)$$

and

$$R(a) = - \sum_{i=1}^{3N} \frac{1}{2} \sum_{k=(a-1)\cdot\text{nstxout}}^{a\cdot\text{nstxout}-1} \left(\frac{\nabla_i U(\mathbf{r}_k)}{\sigma} \right)^2 \Delta t \quad (36)$$

at the same frequency nstxout of the positions. After the simulation, we have reconstructed the complete probability ratio as

$$M_{\tau,x}(\omega) = \exp \left\{ \sum_{a=1}^A I(a) + R(a) \right\}, \quad (37)$$

where $A \in \mathbb{N}$ such that $\tau = n\Delta t = A \cdot \text{nstxout} \cdot \Delta t$. To overcome numerical instabilities caused by Eq. (18), we have used the high precision arithmetic libraries The GNU Multiple Precision Arithmetic Library (GMPLib),⁴⁹ The GNU MPFR Library,⁵⁰ and Eigen.⁵¹

1. Alanine dipeptide

For alanine dipeptide, we ran a reference simulation of length 1 μ s and we saved the positions every nstxout = 100

time steps, corresponding to 0.2 ps. The selected collective variables were the backbone torsion angles ϕ and ψ .

To test the *rerun* method, we have performed a well-tempered metadynamics with the parameters $W = 1.2 \text{ kJ/mol}$, $\sigma_\phi = \sigma_\psi = 0.35 \text{ rad}$, and $\tau_G = 0.2 \text{ ps}$ and bias factor $\lambda = \frac{T+\Delta T}{\Delta T} = 6.0$ of 155 ps. The Gaussian functions were stored on a squared grid with boundaries $-\pi$ and π and a grid spacing of 0.1 for both the torsion angles. We ran simulations of length 20 ns, biased by the metadynamics potential scaled by a factor 0.1, and build an MSM enforcing detailed balance, by discretizing both torsion angles in 36 bins, resulting in $36 \times 36 = 1296$ microstates. The lag-time used for the graphs of the eigenvectors was 100 ps, while the lag-time range for the graphs of the implied time scales was [0: 250] ps. This computational experiment was repeated 20 times to estimate the statistical uncertainty in the implied time scales.

To test the reweighting during the *build-up* phase, we applied a well-tempered metadynamics with the parameters $W = 0.0005 \text{ kJ/mol}$, $\sigma_\phi = \sigma_\psi = 0.5 \text{ rad}$, and $\tau_G = 0.2 \text{ ps}$ and bias factor $\lambda = 6.0$. The simulation length was 500 000 time steps corresponding to 100 ns. The MSM was built by discretizing both torsion angles in 36 bins, resulting in $36 \times 36 = 1296$ microstates and enforcing detailed balance. The lag-time used for the graphs of the eigenvectors was 100 ps, while the lag-time range for the graphs of the implied time scales was [0: 250] ps.

2. Hexapeptide Val-Gly-Val-Ala-Pro-Gly

The hexapeptide was obtained by cutting off the residues from 170 to 177 from the crystal structure of the Ca6 site mutant of Pro-SA-subtilisin⁵² (PDB ID: 3VHQ). We have performed 20 unbiased replica simulations of length 500 ns to build a reference MSM.

The biased collective variable was the end-to-end distance of the peptide, i.e., the distance between the amine nitrogen of residue 1 and the carbonyl carbon of residue 6.

To test the *rerun* method, we have performed a metadynamics simulation of 2 ns, with the parameters $W = 0.1 \text{ kJ/mol}$, $\sigma = 0.02 \text{ nm}$, and $\tau_G = 0.2 \text{ ps}$ to build the bias. Afterward, we have created two sets of simulations biased by the metadynamics potential scaled by a factor 0.1. The first dataset was of ten simulations of length 40 ns and was used to build a single MSM. The second dataset was of ten simulations of length 100 ns and was used to build ten different MSMs.

To test the reweighting during the *build-up* phase, we applied a well-tempered metadynamics with the parameters $W = 0.0005 \text{ kJ/mol}$, $\sigma = 0.02 \text{ nm}$, and $\tau_G = 0.2 \text{ ps}$ and bias factor $\lambda = 6.0$. The simulation length was 100 ns.

In both the cases, the bias was stored on a one-dimensional grid between 0.2 nm and 2.2 nm, with a grid-spacing of 0.03 nm.

The MSM have been built, enforcing detailed balance, by discretizing the collective variable in 50 microstates. The lag-time used for the graphs of the eigenvectors was 200 ps, while the lag-time range for the graphs of the implied time scales was [0: 600] ps.

3. β -hairpin peptide

The β -hairpin structure has been extracted from the immunoglobulin binding domain of streptococcal protein G⁵³ (PDB ID: 1GB1). We have performed 48 simulations of length 350 ns (total simulation time of 16.8 μ s).

Metadynamics has been realized by biasing the three hydrogen-bonds, named r_1 , r_2 , and r_3 , connecting, respectively, the residues 2-15, 4-13, and 6-11. The parameters used to build the Gaussian functions are $W = 0.15$ kJ/mol, $\sigma = 0.1$ nm, and $\tau_G = 1$ ps and bias factor $\lambda = 6.0$. The simulation length was 50 ns.

The bias has been stored on a one-dimensional grid between 0.0 nm and 5.2 nm, with a grid-spacing of 0.03 nm. Afterward, we ran 35 parallel simulations of length 40 ns, biased by the metadynamics potential, scaled by a factor 0.1.

In the β -hairpin peptide, we did not use the metadynamics collective variables to construct the Markov state model but instead used the time-structure based Independent Component Analysis (tICA) method to estimate a two-dimensional subspace from the metadynamics rerun simulations. The input coordinates of for tICA were the time series of the minimal atom root-mean-square distances (minRMSD) to a reference structure, i.e., $\|\mathbf{x}_i(t) - \mathbf{x}_{i,\text{ref}}\|$, where $i = 1, \dots, N$ is the atom index and $\mathbf{x}_i(t)$ are the Cartesian coordinates of atom i at time

t . As a reference structure, we chose the first frame of the trajectory, i.e., $\mathbf{x}_{i,\text{ref}} = \mathbf{x}_i(0)$. The prefix “min” indicates that the atom root-mean-square distances have been measured after a rotational and translational fit has been applied to the structure at time t such that the overall RMSD between the two structures ($\text{RMSD}_{\text{tot}} = \frac{1}{N} \sqrt{\sum_{i=1}^N (\mathbf{x}_i(t) - \mathbf{x}_{i,\text{ref}})^2}$) is minimized. Then, we used the k -means algorithm on the two time-independent coordinates with the largest eigenvalues of the tICA matrix and clustered the data in 50 states. The MSM has been stated on a Voronoi discretization which is generated by the 50 cluster centers, enforcing detailed balance. MSM tICA analysis^{54,55} has been implemented through the package PyEMMA.⁵⁶

IV. RESULTS

A. One-dimensional system

We illustrate the metadynamics/Girsanov-reweighting method on a one-dimensional diffusion process and test how the strength of the bias influences the uncertainty in the reweighted implied time scales. The potential energy function [Eq. (33) and Fig. 1(a)] has three minima at $x = -1.12$, $x = 0.05$, and $x = 1.29$, separated by two barriers located at $x = -0.83$ and $x = 0.61$. The first left MSM eigenvector [Fig. 1(b)] is equal to the Boltzmann distribution. The second eigenvector represents

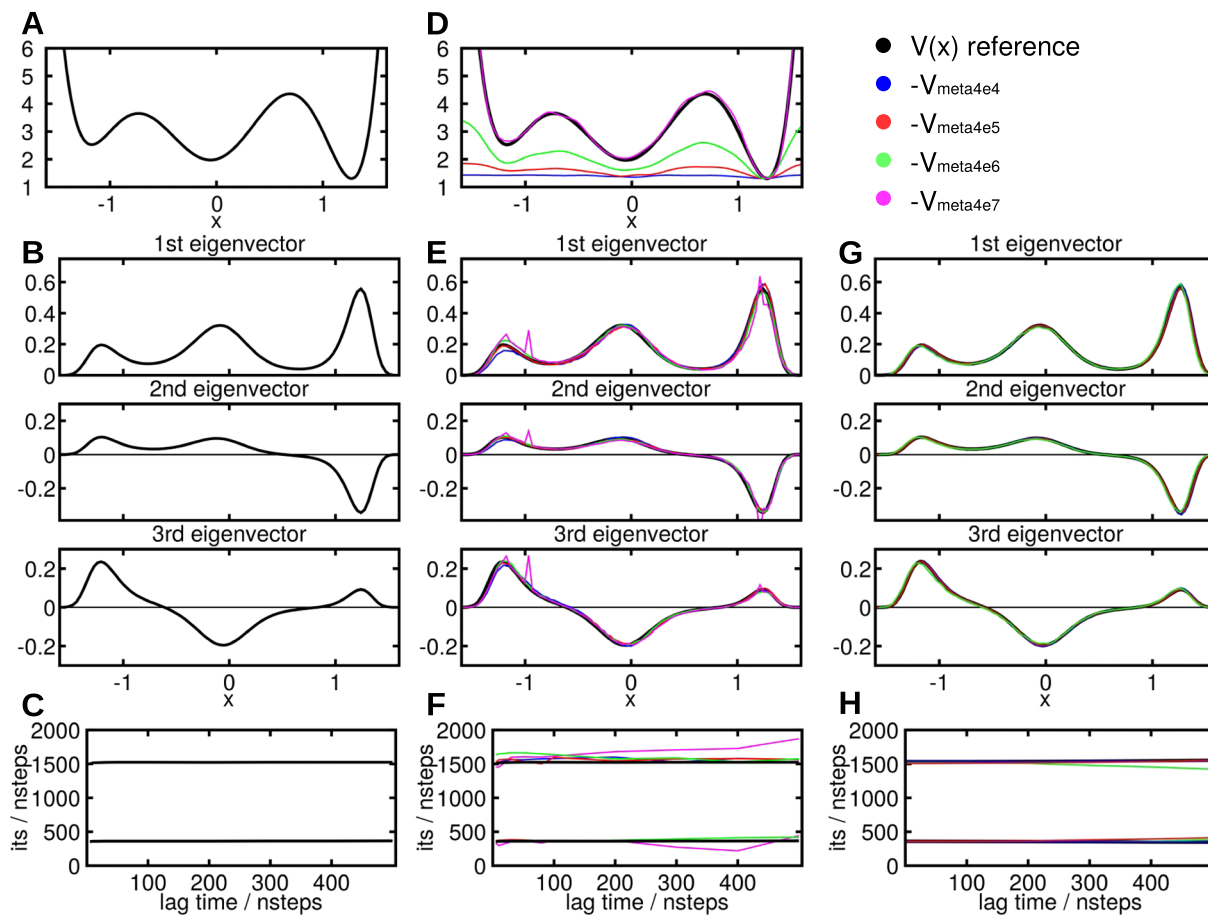


FIG. 1. One-dimensional diffusion process. (a) Potential energy function. (b) First three left MSM eigenvectors. (c) Implied time scales associated with the second and third eigenvector. (d) Free energy profile associated with the metadynamics potential. (e) First three left MSM eigenvectors—rerun. (f) Associated implied time scales—rerun. (g) First three left MSM eigenvectors—build-up. (h) Associated implied time scales—build-up.

the transition across the largest barrier at $x = 0.61$ with an associated implied time scale of 1530 time steps [Figs. 1(b) and 1(c)]. The third eigenvector represents the dynamic exchange between the middle well and the two wells on the sides with an associated implied time scale of 358 time steps [Figs. 1(b) and 1(c)].

The implied-time scale test in Fig. 1(c) shows that the two largest implied time scales of the system are constant, already at very small lag times. This indicates that for the chosen discretization, the discretization error is negligible and the MSM is an excellent approximation of the underlying diffusion process. Thus, any deviation from this reference solution in the metadynamics/Girsanov-reweighting results can be attributed to either statistical uncertainties or to errors due to the reweighting procedure.

Column “Direct simulation” in Table I gives an overview of the statistical uncertainties in the implied time scales for the direct simulation of the process with different simulation lengths: 4e4, 4e5, 4e6, and 4e7 time steps. As expected, increasing the length of the simulation reduces the statistical uncertainties. Note however that the shortest simulation with 4e4 time steps is more than an order of magnitude longer than the slowest implied time scale, yet the statistical uncertainty is still 20%. To decrease the uncertainty to less than 10%, a direct simulation of 4e5 time steps is needed. Due to this slow decrease of the statistical uncertainty with simulation length, statistical uncertainties of 20% and more are quite common in MSMs of molecular systems.⁵⁷

1. Metadynamics/Girsanov reweighting on rerun simulations

We produced four metadynamics potentials $V_{\text{meta}4e4}$, $V_{\text{meta}4e5}$, $V_{\text{meta}4e6}$, and $V_{\text{meta}4e7}$ by writing out $V_{\text{meta}}(s, t)$ [Eq. (5)] at $t = 4e4$, 4e5, 4e6, and 4e7 time steps. We chose a protocol in which the metadynamics potential is build up slowly such that the bias is distributed evenly across the x -axis. Figure 1(d) shows the inverted metadynamics potentials shifted by a constant such that all potentials coincide in the right-hand minimum of the potential energy surface, i.e., $-V_{\text{meta}4e4} + C_{\text{meta}4e4}$, $-V_{\text{meta}4e5} + C_{\text{meta}4e5}$, etc. In the limit of an infinitely long build-up phase, the sum of the metadynamics potential and reference potential should yield a constant potential, i.e., $V(x) + V_{\text{meta}}(x) = C_{\text{meta}}$. Then, up to a constant, the inverted metadynamics potential is equal to the reference potential, i.e., $-V_{\text{meta}}(x) + C_{\text{meta}} = V(x)$. Indeed, the inverted metadynamics potential for a build-up phase of $t = 4e7$ time steps is almost equal to the reference potential [magenta line in Fig. 1(d)]. The build-up phase of $t = 4e4$ time steps yields a very weak metadynamics potential, whereas build-up phases of $t = 4e5$ and $t = 4e6$ time steps yield metadynamics potentials of intermediate strength.

Each of the four metadynamics potentials was used as a constant bias for a new set of simulations. From these biased simulations, we obtained MSMs of the reference system using the Girsanov-reweighting method. For $V_{\text{meta}4e4}$, $V_{\text{meta}4e5}$, and $V_{\text{meta}4e6}$, the slowest MSM eigenfunctions are in excellent agreement with the reference solution [Fig. 1(e)]. For $V_{\text{meta}4e7}$, the eigenvectors deviate in the region of the first minimum in the potential energy surface from the reference solution. The

implied time scale test [Fig. 1(f)] shows that for the reweighted MSMs (as for the reference MSM) the discretization error is negligible for a wide range of lag times. To investigate the statistical uncertainty of the implied time scales, we varied the simulation length of each of the biased simulations between 4e4 and 4e6 time steps (columns “ $V_{\text{meta}4e4}$ ” to “ $V_{\text{meta}4e7}$ ” in Table I). All of the estimates agree within the statistical uncertainty with the corresponding reference values. For each metadynamics potential, increasing the simulation length of the biased simulation decreases the statistical uncertainty, as would be expected.

However, increasing the bias does not necessarily decrease the statistical uncertainty. For a given simulation length, the biases $V_{\text{meta}4e4}$ to $V_{\text{meta}4e6}$ yield similar statistical uncertainties. By contrast, the largest bias $V_{\text{meta}4e7}$ yields much higher statistical uncertainties. The reason for this is that the overall statistical uncertainty is a combination of the number of observed transitions and the variance of the estimator for the path probability ratio $M_{\tau,x}(\omega)$ [Eq. (18)]. This variance increases with the gradient of the bias $\nabla_i U(\mathbf{r})$. Thus, a larger bias increases the number of observed transitions across the largest barrier in the reference system, which reduces the overall statistical uncertainty. But it also generates a larger gradient, which yields a larger variance in the estimator of $M_{\tau,x}(\omega)$. In metadynamics/Girsanov-reweighting, these two effects need to be balanced when choosing the optimal bias. We suggest to use a metadynamics potential which partially compensates the free-energy profile along the collective variables. This can, for example, be achieved by rescaling a metadynamics potential. If the metadynamics potential is fully converged, this is equivalent to using a well-tempered metadynamics potential as a bias [Eq. (7)].

Table I seems to indicate that for a given simulation length, metadynamics/Girsanov-reweighting only marginally improves on the statistical uncertainties compared to the direct simulation. This seems to be an artifact of the one-dimensional system. For higher-dimensional systems, biasing a low-dimensional subspace considerably improved the accuracy of the results compared to the direct simulation.

2. Metadynamics/Girsanov reweighting during the build-up phase

Girsanov reweighting can also be applied to time-dependent biasing potentials. Thus, it can be applied directly to the *build-up phase* of the metadynamics potential. With this strategy, one can omit the subsequent rerun simulation. We reweighted build-up phases of $t = 4e4$, 4e5, and 4e6 time steps to obtain MSMs of the reference system. Both, the reweighted eigenvectors and implied time scales are in excellent agreement with the eigenvectors of the reference system [Fig. 1(g) and Table I]. The uncertainty of the implied time scales is reduced with respect to the direct simulations (Table I).

B. Free energy profile from the reweighted MSM

For a sufficiently long build-up phase, the metadynamics potential converges to minus the free energy F profile along the collective variable $V_{\text{meta}}(s, t \rightarrow \infty) = -F(s) + C$. In praxis, converging this estimate of the free energy profile

often requires very long build-up simulations. With metadynamics/Girsanov reweighting, the free energy profile can be obtained from an unconverged metadynamics potential. From a simulation with a constant, but not a fully converged metadynamics biasing potential or from the build-up phase of the metadynamics potential, an MSM of the reference system is constructed in the space of the collective variables using Girsanov reweighting. The first left eigenvector $l_0(s)$ of this MSM represents the Boltzmann distribution of the reference system,

$$l_0(s) = \pi(s) = \frac{1}{Z} \exp(-\beta F(s)). \quad (38)$$

Thus, the free energy profile can be obtained from

$$F(s) = -\frac{1}{\beta} \log(\pi(s)) + C = -\frac{1}{\beta} \log(l_0(s)) + C, \quad (39)$$

where C is an arbitrary constant. We tested this approach on the one-dimensional system with constant bias $V_{\text{meta}4e6}$. Because the position space of the system and the space of the collective variables are identical in this case, $F(s) = V(x)$. In Fig. 2, the red points represent the free energy profile obtained from the first eigenvector of the reweighted MSM, built on the metadynamics trajectory of length 4e6 time steps. The free energy profile obtained in this way fully matches with the expected potential energy function, and it considerably improved the free energy profile obtained by converting the corresponding metadynamics potential $V_{\text{meta}4e6}$ (Fig. 2, green line).

C. Alanine dipeptide

As a first molecular test system for the metadynamics/Girsanov-reweighting method, we used alanine dipeptide (Ac-Ala-NHMe). We built an MSM of alanine dipeptide on the space of the backbone torsion angles ϕ and ψ from 1 μ s direction simulation of alanine dipeptide in implicit water as a reference. Figure 4(a) (first row) shows the well-known dominant left MSM eigenvectors:⁵⁷ the first eigenvector is the stationary distribution with the typical conformational states (β region, L_α region, and R_α region); the second eigenvector represents the transition around the ϕ torsion angle corresponding to a kinetic exchange between the L_α -minimum and the α -helix and β -sheet minima; the third eigenvector represents the torsion around ψ corresponding to a kinetic exchange between the β region and the R_α -helical conformation. The associated time scales of the two transitions are $t_1 = 2.8$ ns and $t_2 = 27$ ps. The implied time scales are approximately constant, indicating that the MSM is a good approximation of the dynamics

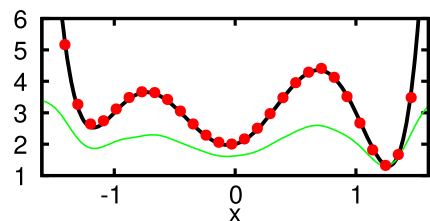


FIG. 2. One-dimensional diffusion process. (Black) Potential energy function; (green) free energy profile associated with $V_{\text{meta}4e6}$; (red dots) free energy profile obtained from the first eigenvector of a reweighted MSM built from a metadynamics simulation of 4e6 time steps.

and that the discretization error is small [Fig. 4(b), green lines].

1. Metadynamics/Girsanov reweighting on rerun simulations

Next, we performed a well-tempered metadynamics simulation of 155 ps, where we chose the ϕ and ψ backbone torsion angles as collective variables. Figure 3(a) shows the build-up of the metadynamics potential for $0 \leq t \leq 150$ ps. After 150 ps, the metadynamics potential is almost fully converged in the ϕ -torsion angle and reasonably well-converged in the ψ -torsion angle. Note that we use the metadynamics bias to speed up the sampling in the collective variables and not to measure the free-energy profile of the system. Thus, full convergence is not required. On the contrary, our experiments with the one-dimensional diffusion process had shown that a fully converged metadynamics potential causes a large variance in the estimator for path probability ratio $M_{\tau,x}(\omega)$. We therefore rescaled the final metadynamics potential by a

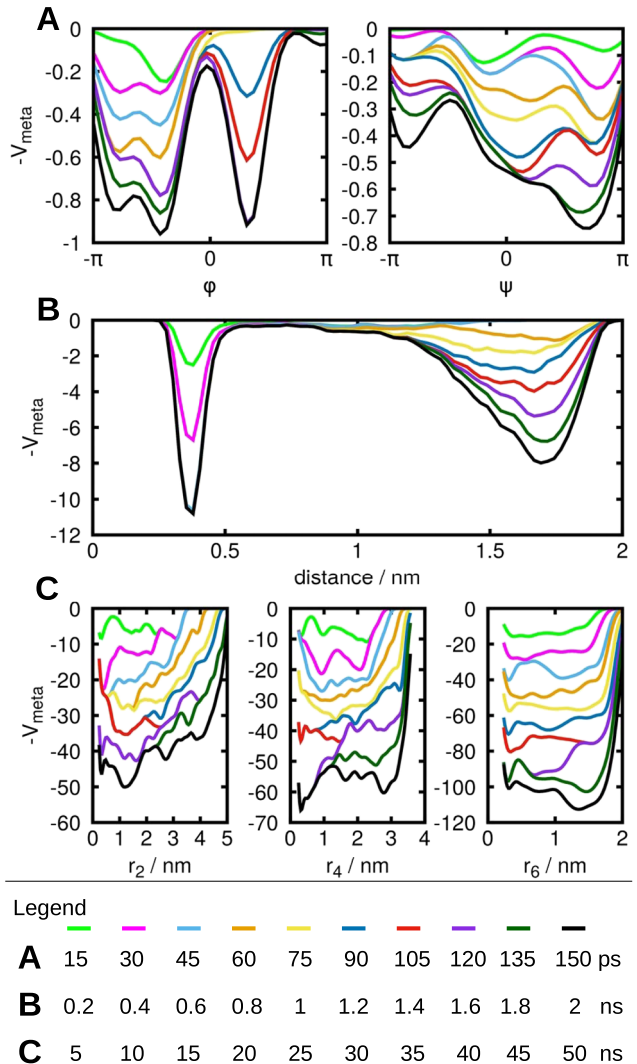


FIG. 3. Time evolution of the metadynamics potentials on the relevant coordinates. (a) Alanine dipeptide, potential every 15 ps, from 0 ps (green) to 150 ps (black). (b) VGVAPG hexapeptide, potential every 200 ps, from 0 ps (green) to 2000 ps (black). (c) β -hairpin, potential every 5 ns, from 0 ns (green) to 50 ns (black).

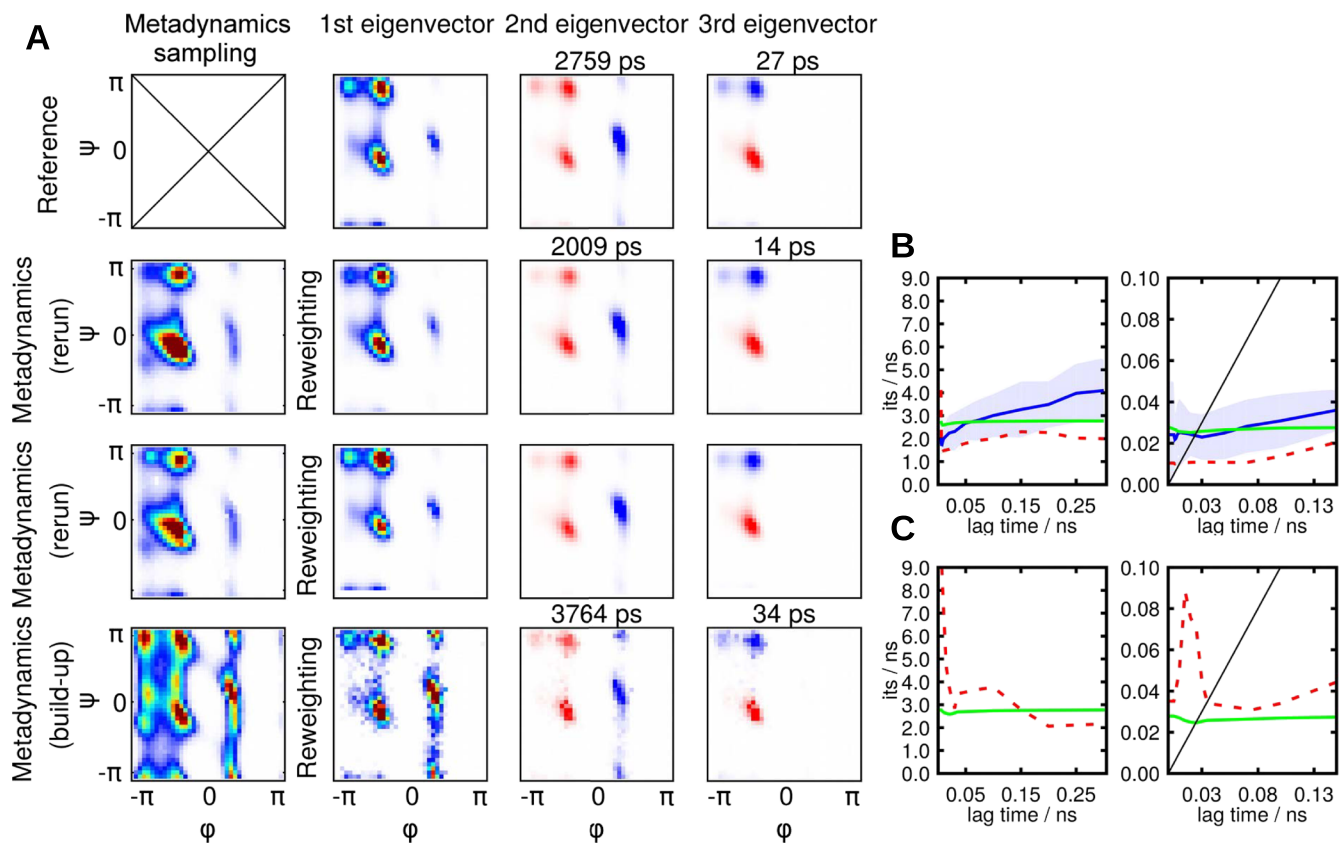


FIG. 4. Alanine dipeptide. (a) First three left MSM eigenvectors. 1st row: reference; 2nd and 3rd rows: reweighting after two independent rerun simulations; 4th row: reweighting during the build-up phase. (b) Implied time scales associated with the second and third eigenvector, rerun method. Green: reference, blue: average and standard deviation over twenty reweighted trajectories red: reweighting of a single trajectory. (c) Implied time scales associated with the second and third eigenvector, build-up method. Green: reference, red: reweighting.

factor 0.1 and produced rerun simulations of 20 ns each at this rescaled potential. This computer experiment was repeated twenty times to account for the statistical uncertainty in the reweighted MSMs. The Boltzmann distribution obtained from the biased simulations is shown in Fig. 4(a) for two different rerun simulations (second and third row, first column). The sampling of the $\phi - \psi$ space is increased [compared to Fig. 4(a), first row, second column], but the overall structure of the underlying reference potential is still clearly visible. To get an estimate of the speed-up of the rerun metadynamics simulation compared to the unbiased simulation, we estimated an MSM from the rerun trajectory without applying Girsanov reweighting. The slowest process is still the torsion around ϕ , but the associated time scale is now 780 ps (data not shown) compared to 2.8 ns in the unbiased simulation. Thus, although we used a moderate bias, we still gain a speed-up by roughly a factor of 4.

Reweighting the rerun metadynamics simulations yielded the dominant left eigenvectors shown in Fig. 4(a) (second and third rows) that are in excellent agreement with the eigenvectors of the reference system. However, the associated implied time scales from single trajectories or aggregated trajectories are lower and less smooth than the implied time scale plot of the direct simulation [Fig. 4(b), red dashed line]. The blue line in Fig. 4(b) shows the average and standard deviation over a set of twenty reweighted MSMs, which is in good agreement with the reference model. Thus, the metadynamics/

Girsanov-reweighting yields the correct expected values and the non-smoothness of the implied time scale plots is due to statistical uncertainty, i.e., the variance of the estimator.

2. Metadynamics/Girsanov reweighting during the build-up phase

We also constructed reweighted MSMs from the build-up phase of the metadynamics potential. However, we chose a much smaller height W for the Gaussians [Eq. (5)] such that the growth of the metadynamics potential was slower than the slowest time scale of the unbiased system. The build-up simulation for the metadynamics potential was run for 100 ns. The corresponding sampling of the $\phi - \psi$ space is shown in Fig. 4(a) (third row, first column). Reweighting the build-up metadynamics simulations yielded the dominant left MSM eigenvectors shown in Fig. 4(a) (third row). They are in good agreement with the dominant MSM eigenvectors of the unbiased system; in particular, they correspond to the same conformational transitions. The population of the L_α -region is overestimated, and overall the eigenvectors are “noisier” than those estimated from the metadynamics rerun simulation. The estimated slowest implied time scale is 3.8 ns.

D. Hexapeptide Val-Gly-Val-Ala-Pro-Gly

As non-trivial molecular system for which we can still generate a reference solution, we chose the hexapeptide

Val-Gly-Val-Ala-Pro-Gly (VGVAPG). The peptide has charged termini and its slowest process is the opening and closing of the salt-bridge between the positively charged N-terminus and the negatively charged C-terminus [Fig. 5(b)]. Correspondingly, we chose the distance between the nitrogen atom of the N-terminus and the carboxyl-carbon of the C-terminus as a collective variable for the metadynamics potential as well as for the MSM.

We performed 10 μ s of direct simulations of VGVAPG and constructed a reference MSM. The dominant left MSM eigenvectors are shown as green lines in Figs. 5(c) and 5(e). The first eigenvector represents the Boltzmann distribution along the reaction coordinates, which has two maxima. When the hexapeptide is in the closed conformation, the distance between the nitrogen atom and the carbon atom is around 0.25 nm. When the hexapeptide is in the open conformation, the distance between the backbone termini varies between 0.6 and 1.8 nm. The slowest process is the exchange between these two conformations and is associated with an implied time scale of about 5 ns [Fig. 5(d), green line]. The second slowest process is the exchange between open but relatively compact conformations and conformations at the ends of the distance distribution, i.e., very extended conformations or closed conformations. It is associated with an implied time scale of about 1 ns.

1. Metadynamics/Girsanov reweighting on rerun simulations

We obtained an almost fully converged metadynamics potential after 2 ns of metadynamics build-up simulation [Fig. 3(b)]. As for the one-dimensional case and the alanine-dipeptide, a fully converged metadynamics potential is not the optimal bias for our purpose; thus, we rescaled the bias by a factor 0.1 [blue and green lines in Fig. 5(a)] and then we ran twenty biased simulations of 40 ns to 100 ns. The left eigenvectors of the reweighted MSMs built from single trajectories are in excellent agreement with the eigenvectors of the reference system [Fig. 5(c), respectively, black and green lines]. Also, the reweighted implied time scales, from a MSM built on an aggregated trajectory (400 ns in total), match those of the reference system for lag times of $\tau \leq 300$ ps [Fig. 5(d), red dashed line]. For larger lag times, they drift to large values. The likely reason for this behavior is that the variance of the estimator of $M_{\tau,x}(\omega)$ increases with the length of τ , i.e., with the number of terms in the sum $\sum_{k=0}^n$ in Eq. (18). The blue line shows the average and standard deviation of a set of ten reweighted MSMs each estimated from a trajectory of 100 ns. As for alanine dipeptide, also here the expected value is in good agreement with the reference model.

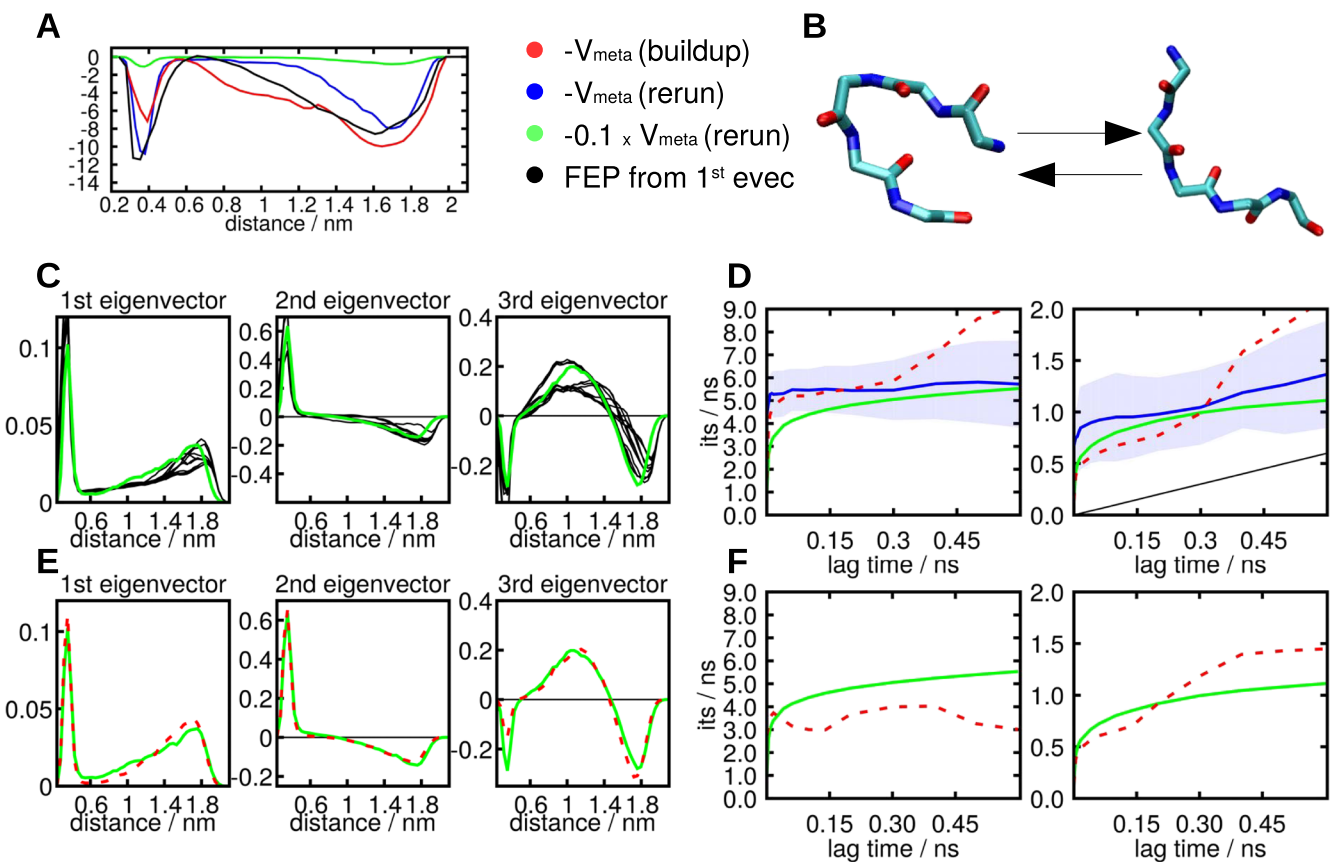


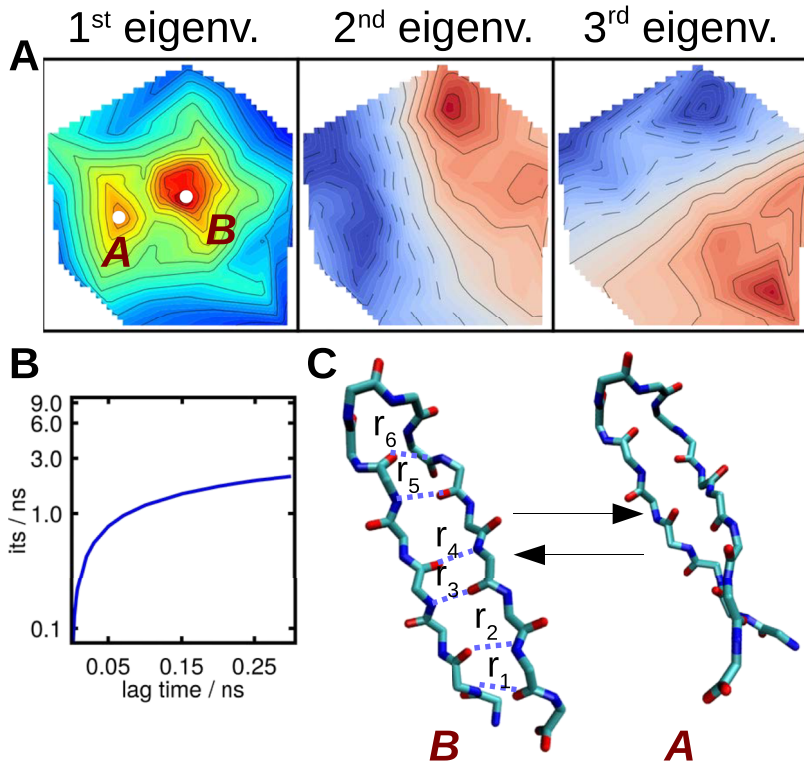
FIG. 5. Hexapeptide VGVAPG. (a) Free energy profiles. (b) Open and closed conformations of VGVAPG. (c) First three left MSM eigenvectors, rerun method. Green: reference, Black: reweighting of ten trajectories. (d) First two implied time scales, rerun method. Green: reference, blue: average over ten reweighted trajectories, red: reweighting of a single trajectory. (e) and (f) First three left MSM eigenvectors and associated implied time scales, build-up method. Green: reference, red: reweighting.

2. Metadynamics/Girsanov reweighting during the build-up phase

To reweight the build-up phase of the metadynamics potential, we chose a slow build-up mode: 100 ns of well-tempered metadynamics simulation. The free-energy profile associated with the final metadynamics potential is shown in red in Fig. 5(a). Girsanov reweighting of this simulation yields eigenvectors which are in very good agreement with the reference MSM [Fig. 5(e)]. Only the population of the closed conformation is slightly under-estimated. The associated implied time scales are in reasonable agreement with the reference solution. Interestingly, the implied time scale plots do not diverge for large lagtimes, as it was the case in the metadynamics/Girsanov-reweighting models of the rerun simulation.

E. β -hairpin peptide

As a last example, we chose the β -hairpin from the immunoglobulin binding domain of streptococcal protein G.⁵³ The rearrangement of the hydrogen-bond pattern in the β -hairpin is a very slow process. In 16.8 μ s of direct simulation of the β -hairpin peptide, we did not observe a single opening event. We nonetheless analyzed the dynamics of this simulation by constructing a MSM in the tICA^{54,55} space of the closed peptide (Fig. 6). The most frequent structures are a hairpin laying on a plane and a twisted hairpin along the axis of the H-bonds [Fig. 6(c)]. Thus the only kinetic exchange revealed by the direct simulation is torsion of the closed β -hairpin associated with a time scale of 2.5 ns [Fig. 6(b)]. Note that this MSM is not a reference solution since the slowest process—the rearrangement of the hydrogen bonds—has not been observed in the direct simulation.



1. Metadynamics/Girsanov reweighting on rerun simulations

We have built a metadynamics potential in the space of the distances r_2 , r_4 , and r_6 [Fig. 6(c)] by conducting 50 ns of well-tempered metadynamics. From the time evolution of the metadynamics potential on the relevant coordinates r_2 and r_4 , we deduce that the bias is far from convergence [Fig. 3(c)]. Indeed, the metadynamics potential does not relax toward a constant function, but it is subjected to relevant fluctuations. Moreover, we cannot distinguish basins of metastable states. Only the potential on the distance r_6 relaxed toward an almost stable profile that suggests the existence of two metastable regions. On the other hand, during this build-up phase, the β -hairpin did not only open but in fact sampled completely extended structures. As before, we scaled the obtained potential by a factor of 0.1 and used it as a constant bias in 1.4 μ s of metadynamics rerun simulations.

To gauge the sampling in this biased simulation, we constructed tICA-MSMs without reweighting [Fig. 7(a), top row]. Additionally to the planar hairpin (structure A) and the twisted hairpin (structure B), we found a half-open structure C in which the hydrogen bonds toward the end of the β -hairpin are broken [Fig. 7(d)]. The most extended conformation sampled by the metadynamics simulation is the structure D [Fig. 7(d)]. The eigenvectors of the reweighted MSMs are shown in the bottom line of Fig. 7(a). The extended structure D is now located on a barrier, while structures A, B, and C are still minima. The slowest process is the exchange between the half-open structure D and the two fully formed β -hairpin structures. The associated implied time scale is in the range of 100 ns to 1 μ s [Fig. 7(b)]. The second slowest process is the exchange between the planar β -hairpin (structure A) and the twisted

FIG. 6. β -hairpin, reference simulation. (a) First three tICA eigenvectors. (b) Implied time scale associated with the second tICA eigenvector. (c) Conformations A and B.

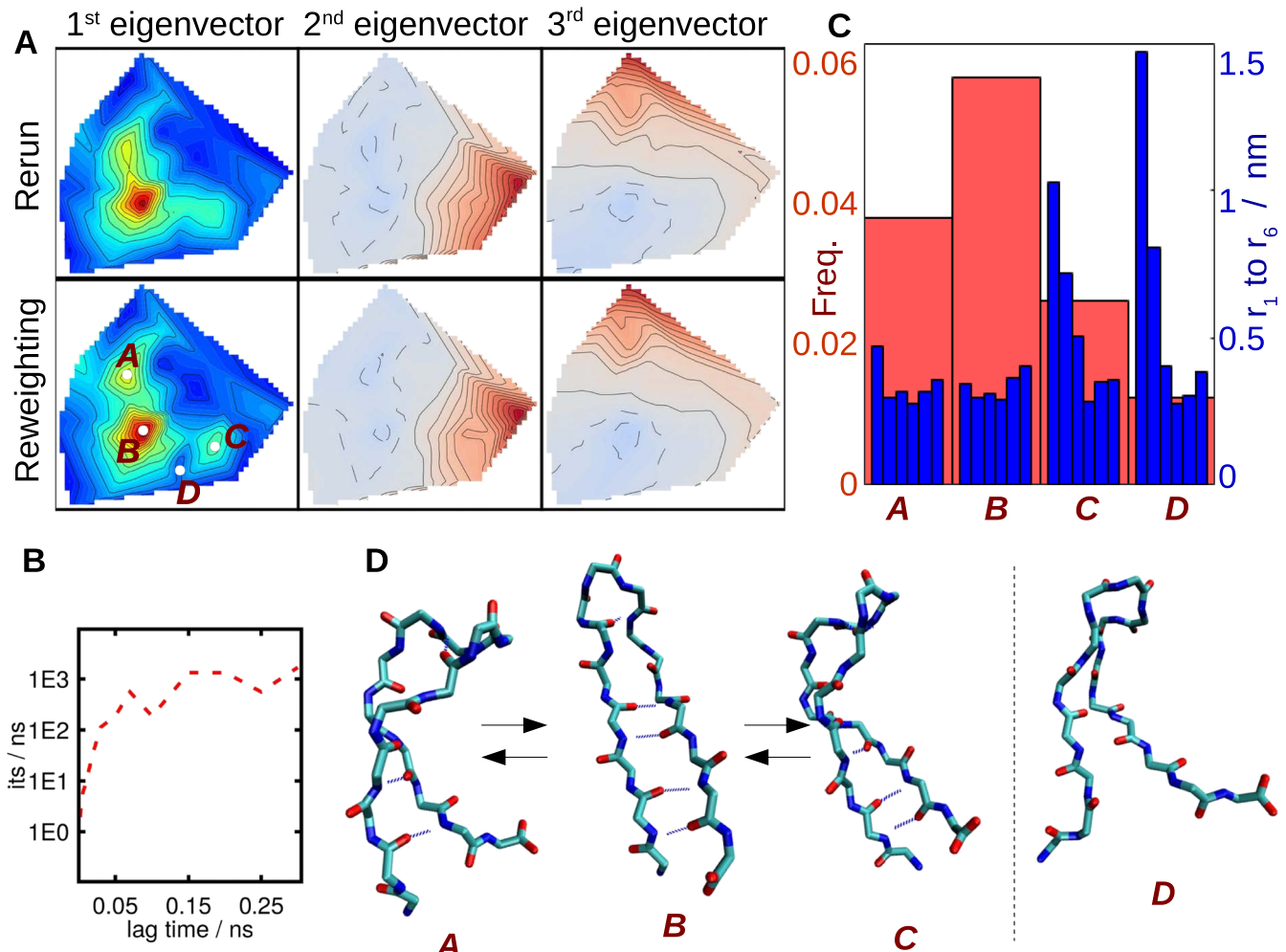


FIG. 7. β -hairpin, metadynamics simulation. (a) First three tICA eigenvectors. First row: rerun simulation, second row: rerun reweighting. (b) Implied time scale associated with the second eigenvector (reweighting). (c) Frequency of the structures A, B, C, and D (red, left axis); r_1 to r_6 distances in nm, blue columns from left to right (right axis). (d) Conformations A, B, C, and D.

hairpin (structure *B*). Figure 6(c) shows the reweighted relative population of the four structures (red bars) and the distance of the hydrogen-bonds r_1 , r_2 , r_3 , r_4 , r_5 , and r_6 connecting, respectively, the residues 1-16, 2-15, 3-14, 4-13, 5-12, and 6-11 (blue bars).

V. DISCUSSION AND CONCLUSION

We have presented an application of the Girsanov reweighting scheme^{38,39} to metadynamics,³⁻⁶ to recover the correct dynamic properties of a molecular system from an enhanced sampling simulation. We have studied two possible strategies. In the first one, that we called *rerun*, we have first built a metadynamics bias, then we have rerun a simulation with the bias as a constant function and we applied the Girsanov reweighting on the trajectory produced by the second simulation. In the second strategy, we have applied the Girsanov reweighting directly during the *build up* phase of the metadynamics simulation, exploiting the validity of the Girsanov theorem for time-dependent perturbations. Both approaches recovered the correct unbiased dynamics for a wide range of systems.

The major difference between the Girsanov reweighting method and other dynamic reweighting methods³²⁻³⁶ is that the probability density of each possible path of length τ connecting two points $\mathbf{x}_0 = \mathbf{x}$ and $\mathbf{x}_n = \mathbf{y}$ is reweighted and not the MSM transition probability as such. To reweight path probability densities, two prerequisites need to be fulfilled: (*i*) the equation of motion of the molecular systems needs to contain a normal random noise term (Langevin dynamics or Brownian dynamics); (*ii*) the gradient $\nabla_i U(\mathbf{r})$ and the random numbers need to be evaluated for each integration time step to obtain the path probability ratio $M_{\tau,x}(\omega)$ [Eq. (18)]. The first condition is easily satisfied by using a Langevin thermostat to maintain the temperature. The random forces from this thermostat then serve as the random noise term.³⁹ The second condition, in principle, requires that the two properties are written to file for each integrator time step, which is not practical. However, if the bias is known for each time step of the simulation, as in metadynamics, two properties can be evaluated on the fly and interim results for $M_{\tau,x}(\omega)$ are written to file at the same frequency as the coordinates. For this approach, the integrator of the MD simulation program needs to be modified

accordingly,³⁹ which is unproblematic in modular MD codes, such as OpenMM.⁴⁵

Thus in practice, Girsanov reweighting is not an analysis method that can be used independent of the MD simulation, but it is intertwined with the MD simulation program. This slightly more complex set-up pays off in two ways. First, one does not need to assume that the system is in local equilibrium within a state B_i before it transitions to a state B_j . Second, Girsanov reweighting can be used to reweight arbitrary time-lagged correlation functions [Eq. (2)] and is not limited to transition counts. In particular, it can be used directly to reweight Markov models with advanced discretization methods, such as tICA,^{54,55} variational Markov models^{58,59} or core-set models.^{60,61} Girsanov reweighting is closely related to the Onsager-Machlup action^{62–66} and path reweighting methods for parallel tempering simulations.^{29–31}

A critical assumption in metadynamics is that the collective variables, along which the metadynamics potential is built up, are aligned with the slow conformational transitions of the system such that the sampling in the degrees of freedom orthogonal to the collective variables is fast. This condition also needs to be fulfilled when applying Girsanov reweighting to a metadynamics simulation. In this contribution, we have therefore chosen systems with known collective variables. Once a suitable set of collective variables for the metadynamics simulations is known, it can be re-used as reaction coordinates for the discretization of the MSM, thus yielding MSMs with a small discretization error.

It is important to point out that the variance of the Girsanov reweighting estimator is a critical factor in the metadynamics/Girsanov reweighting method. It depends on the gradient of the bias, the length of the paths τ (i.e., the MSM lag time), and the number of paths of length τ (i.e., the sampling in the rerun simulations). The gradient of the bias can be controlled by scaling the metadynamics potential. Our results have shown that a fully converged metadynamics potential is usually not the optimal choice but that suitable balance between the speed-up of the simulation and suitable variance of the Girsanov reweighting estimator can be achieved by rescaling the potential by a factor of 0.1. The lag time τ can be decreased by reducing the MSM discretization error. The fact that a metadynamics simulation is only possible if a suitable set of collective variables is known simplifies the search for a good discretization drastically. The lag time could further be reduced by using advanced discretization methods^{54,55,58–61} in the space of the collective variables. Finally, the length of the rerun simulation is limited by the available computer resources and by the obvious requirement that computational costs of a rerun simulation should be lower than those of a direct simulation.

In conclusion, metadynamics/Girsanov-reweighting is a valuable tool for obtaining dynamic properties, including MSMs and Markov models with advanced discretizations, from enhanced sampling simulations. Our results show that metadynamics/Girsanov-reweighting considerably decreases the computational costs of Markov models, and we expect that this will make Markov models amenable to a wider circle of scientists.

ACKNOWLEDGMENTS

This research has been funded by Deutsche Forschungsgemeinschaft (DFG) through Grant No. CRC 1114 *Scaling Cascades in Complex Systems*, B05 *Origin of the scaling cascades in protein dynamics*.

- ¹Y. Sugita and Y. Okamoto, *Chem. Phys. Lett.* **329**, 261 (2000).
- ²M. Souaille and B. Roux, *Comput. Phys. Commun.* **135**, 40–57 (2001).
- ³T. Huber, A. Torda, and W. van Gunsteren, *J. Comput.-Aided Mol. Des.* **8**, 695 (1994).
- ⁴A. Laio and M. Parrinello, *Proc. Natl. Acad. Sci. U. S. A.* **99**, 12562 (2002).
- ⁵A. Barducci, G. Bussi, and M. Parrinello, *Phys. Rev. Lett.* **100**, 020603 (2008).
- ⁶M. Bonomi, D. Branduardi, C. Camilloni, and G. Bussi, *Comput. Phys. Commun.* **185**, 604 (2014).
- ⁷P. G. Bolhuis, D. Chandler, C. Dellago, and P. L. Geissler, *Annu. Rev. Phys. Chem.* **53**, 291 (2002).
- ⁸A. K. Faradjian and R. Elber, *J. Chem. Phys.* **120**, 10880 (2004).
- ⁹R. B. Best and G. Hummer, *Proc. Natl. Acad. Sci. U. S. A.* **102**, 6732 (2005).
- ¹⁰R. Hegger and G. Stock, *J. Chem. Phys.* **130**, 034106 (2009).
- ¹¹P. Faccioli, A. Lonardi, and H. Orland, *J. Chem. Phys.* **133**, 045104 (2010).
- ¹²C. Schütte, A. Fischer, W. Huiszinga, and P. Deuflhard, *J. Comput. Phys.* **151**, 146 (1999).
- ¹³C. Schütte, W. Huiszinga, and P. Deuflhard, ZIB Report SC-99-36, 1999.
- ¹⁴P. Deuflhard, W. Huiszinga, A. Fischer, and C. Schütte, *Linear Algebra Appl.* **315**, 39 (2000).
- ¹⁵W. C. Swope, J. W. Pitera, F. Suits, M. Pitman, M. Eleftheriou, B. G. Fitch, R. S. Germain, A. Rayshubski, T. J. C. Ward, Y. Zhestkov, and R. Zhou, *J. Phys. Chem. B* **108**, 6582 (2004).
- ¹⁶J. D. Chodera, N. Singh, V. S. Pande, K. A. Dill, and W. C. Swope, *J. Chem. Phys.* **126**, 155101 (2007).
- ¹⁷N.-V. Buchete and G. Hummer, *J. Phys. Chem. B* **112**, 6057 (2008).
- ¹⁸J.-H. Prinz, H. Wu, M. Sarich, B. Keller, M. Senne, M. Held, J. D. Chodera, C. Schütte, and F. Noé, *J. Chem. Phys.* **134**, 174105 (2011).
- ¹⁹B. Keller, X. Daura, and W. F. Van Gunsteren, *J. Chem. Phys.* **132**, 074110 (2010).
- ²⁰B. Keller, P. Hünenberger, and W. F. van Gunsteren, *J. Chem. Theory Comput.* **7**, 1032 (2011).
- ²¹V. A. Voelz, G. R. Bowman, K. A. Beauchamp, and V. S. Pande, *J. Am. Chem. Soc.* **132**, 1526 (2010).
- ²²G. D. Fabritiis, N. Stanley, and S. Esteban-martín, *Nat. Commun.* **5**, 5272 (2014).
- ²³G. R. Bowman, E. R. Bolin, K. M. Hart, B. C. Maguire, and S. Marqusee, *Proc. Natl. Acad. Sci. U. S. A.* **112**, 2734 (2015).
- ²⁴N. Plattner and F. Noé, *Nat. Commun.* **6**, 7653 (2015).
- ²⁵L. Zhang, I. C. Unarta, P. P.-H. Cheung, G. Wang, D. Wang, and X. Huang, *Acc. Chem. Res.* **49**, 698 (2016).
- ²⁶J. Witek, B. G. Keller, M. Blatter, A. Meissner, T. Wagner, and S. Riniker, *J. Chem. Inf. Model.* **56**, 1547 (2016).
- ²⁷M. Biswas, B. Lickert, and G. Stock, *J. Chem. Phys. B* **122**, 5508 (2018).
- ²⁸G. R. Bowman, D. L. Ensign, and V. S. Pande, *J. Chem. Theory Comput.* **6**, 787–794 (2010).
- ²⁹J.-H. Prinz, J. D. Chodera, V. S. Pande, W. C. Swope, J. C. Smith, and F. Noé, *J. Chem. Phys.* **134**, 244108 (2011).
- ³⁰J. D. Chodera, W. C. Swope, F. Noé, J.-H. Prinz, M. R. Shirts, and V. S. Pande, *J. Chem. Phys.* **134**, 244107 (2011).
- ³¹D. D. L. Minh and J. D. Chodera, *J. Chem. Phys.* **131**, 134110 (2009).
- ³²H. Wu, A. S. J. S. Mey, E. Rosta, and F. Noé, *J. Chem. Phys.* **141**, 214106 (2014).
- ³³H. Wu, F. Paul, C. Wehmeyer, and F. Noé, *Proc. Natl. Acad. Sci. U. S. A.* **113**, E3221 (2016).
- ³⁴E. Rosta and G. Hummer, *J. Chem. Theory Comput.* **11**, 276 (2014).
- ³⁵P. Tiwary and M. Parrinello, *Phys. Rev. Lett.* **111**, 230602 (2013).
- ³⁶R. Casasnovas, V. Limongelli, P. Tiwary, P. Carloni, and M. Parrinello, *J. Am. Chem. Soc.* **139**, 4780 (2017).
- ³⁷B. Øksendal, *Stochastic Differential Equations: An Introduction with Applications*, 6th ed. (Springer Verlag, Berlin, 2003).
- ³⁸C. Schütte, A. Nielsen, and M. Weber, *Mol. Phys.* **113**, 69 (2015).

- ³⁹L. Donati, C. Hartmann, and B. G. Keller, *J. Chem. Phys.* **146**, 244112 (2017).
- ⁴⁰J. Quer, L. Donati, and B. G. Keller, *SIAM J. Sci. Comput.* **40**, A653–A670 (2017).
- ⁴¹D. Branduardi, G. Bussi, and M. Parrinello, *J. Chem. Theory Comput.* **8**, 2247–2254 (2002).
- ⁴²F. Marinelli, F. Pietrucci, A. Laio, and S. Piana, *PLoS Comput. Biol.* **5**, e1000452 (2009).
- ⁴³M. Bonomi, A. Barducci, and M. Parrinello, *J. Comput. Chem.* **5**, 1 (2009).
- ⁴⁴P. Tiwary and M. Parrinello, *J. Phys. Chem. B* **119**, 736–742 (2014).
- ⁴⁵P. Eastman, M. S. Friedrichs, J. D. Chodera, R. J. Radmer, C. M. Bruns, J. P. Ku, K. A. Beauchamp, T. J. Lane, L.-P. Wang, D. Shukla, T. Tye, M. Houston, T. Stich, C. Klein, M. R. Shirts, and V. S. Pande, *J. Chem. Theory Comput.* **9**, 461 (2013).
- ⁴⁶J. A. Maier, C. Martinez, K. Kasavajhala, L. Wickstrom, K. E. Hauser, and C. Simmerling, *J. Chem. Theory Comput.* **11**, 3696 (2015).
- ⁴⁷A. Onufriev, D. Bashford, and D. A. Case, *Proteins* **55**, 383 (2004).
- ⁴⁸J. A. Izquierre, C. R. Sweet, and V. S. Pande, *Pac. Symp. Biocomput.* **15**, 240 (2010).
- ⁴⁹T. Granlund and GMP Development Team, *GNU MP: The GNU Multiple Precision Arithmetic Library*, 5th ed. (Free Software Foundation, 2012), <http://gmplib.org/>.
- ⁵⁰L. Fousse, G. Hanrot, V. Lefèvre, P. Pélissier, and P. Zimmermann, *ACM Trans. Math. Software* **33**, 13:1 (2007).
- ⁵¹G. Guennebaud, J. Benoît *et al.*, Eigen v3, <http://eigen.tuxfamily.org>, 2010.
- ⁵²R. Uehara, Y. Takeuchi, S. Tanaka, K. Takano, Y. Koga, and S. Kanaya, *Biochemistry* **51**, 5369 (2012).
- ⁵³A. Gronenborn, D. Filpula, N. Essig, A. Achari, M. Whitlow, P. Wingfield, and G. Clore, *Science* **253**(5020), 657 (1991).
- ⁵⁴C. R. Schwantes and V. S. Pande, *J. Chem. Theory Comput.* **9**, 2000 (2013).
- ⁵⁵G. Perez-Hernandez, T. Paul Giorgino, G. De Fabritiis, and F. Noé, *J. Chem. Phys.* **139**, 015102 (2013).
- ⁵⁶M. K. Scherer, B. Trendelkamp-Schroer, F. Paul, G. Pérez-Hernández, M. Hoffmann, N. Plattner, C. Wehmeyer, J.-H. Prinz, and F. Noé, *J. Chem. Theory Comput.* **11**, 5525 (2015).
- ⁵⁷F. Vitalini, A. S. J. S. Mey, F. Noé, B. G. Keller, F. Vitalini, A. S. J. S. Mey, F. Noé, and B. G. Keller, *J. Chem. Phys.* **142**, 084101 (2015).
- ⁵⁸F. Nüske, B. Keller, G. Perez-Hernandez, A. S. J. S. Mey, and F. Noé, *J. Chem. Theory Comput.* **10**, 1739 (2014).
- ⁵⁹F. Vitalini, F. Noé, and B. G. Keller, *J. Chem. Theory Comput.* **11**, 3992 (2015).
- ⁶⁰C. Schütte, F. Noé, J. Lu, M. Sarich, and E. Vanden-Eijnden, *J. Chem. Phys.* **134**, 204105 (2011).
- ⁶¹O. Lemke and B. G. Keller, *J. Chem. Phys.* **145**, 164104 (2016).
- ⁶²L. Onsager and S. Machlup, *Phys. Rev.* **91**, 1501 (1953).
- ⁶³T. B. Woolf, *Chem. Phys. Lett.* **289**, 433 (1998).
- ⁶⁴D. M. Zuckerman and T. B. Woolf, *J. Chem. Phys.* **111**, 9475 (1999).
- ⁶⁵D. M. Zuckerman and T. B. Woolf, *Phys. Rev. E* **63**, 016702 (2000).
- ⁶⁶C. Xing and I. Andricioaei, *J. Chem. Phys.* **124**, 034110 (2006).